

Cell Surface Engineering with Polyelectrolyte Multilayer Thin Films

John T. Wilson,^{†,‡} Wanxing Cui,[‡] Veronika Kozlovskaya,[§] Eugenia Kharlampieva,[§] Di Pan,[⊥] Zheng Qu,[†] Venkata R. Krishnamurthy,[‡] Joseph Mets,[†] Vivek Kumar,[†] Jing Wen,[‡] Yuhua Song,[⊥] Vladimir V. Tsukruk,[§] and Elliot L. Chaikof^{*,†,‡,§,||,±}

[†]Wallace H. Coulter Department of Biomedical Engineering, Georgia Institute of Technology and Emory University School of Medicine, Atlanta, Georgia 30332, United States

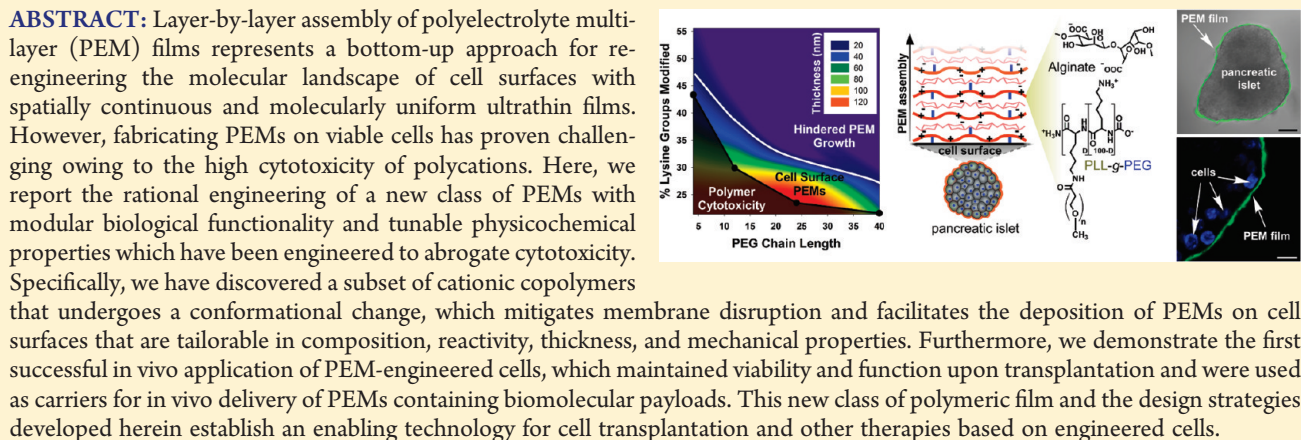
[‡]Department of Surgery, Emory University School of Medicine, Atlanta, Georgia 30322, United States

[§]School of Materials Science and Engineering and ^{||}School of Chemical and Biomolecular Engineering, Georgia Institute of Technology, Atlanta, Georgia 30332, United States

[⊥]Department of Biomedical Engineering, University of Alabama at Birmingham, Birmingham, Alabama 35294, United States

[±]Department of Surgery, Beth Israel Deaconess Medical Center and the Wyss Institute for Biologically Inspired Engineering at Harvard University, Boston, Massachusetts 02115, United States

S Supporting Information



INTRODUCTION

The cell surface is among the most sophisticated materials evolved in nature and its composition defines its capacity to exquisitely regulate immensely diverse physical and chemical processes fundamental to many biological phenomena. Hence, re-engineering the molecular features of cell and tissue surfaces by introducing exogenously derived molecules and nanoscale materials alongside native constituents provides a powerful tool for manipulating processes governed by cell surface molecules and controlling interactions between cells and their environment. Cell surface engineering^{1–13} has been used to introduce reactive handles,¹ proteins and peptides,^{11,14,15} carbohydrates,¹⁶ nucleic acids,^{12,17} and synthetic nanoparticles and polymers^{2,4} to the complex biochemical milieu of the cell surface through genetic, metabolic, chemical, and physical approaches. While genetic and metabolic approaches have proven vital to elucidating cellular processes, their molecular repertoire is typically limited to the natural canon of available molecules and/or cellular biochemical pathways and, hence, are not amenable to modifying cell surfaces with a large class of molecules and materials. Other strategies,

such as covalent tethering to reactive cell surface moieties or incorporation of amphiphilic molecules into plasma membranes, expand options for surface modification, but they can perturb cell physiology in undesired manners^{7,18} and, as monomolecular films, offer limited opportunities for interfacial engineering.

Over the past two decades the assembly of polyelectrolyte multilayer (PEM) films has emerged as a powerful and versatile, yet facile, bottom-up approach for engineering diverse organized thin films, both supported and freely standing, with surface morphology, composition, as well as biological and physicochemical properties readily tailored through assembling routines.^{19–24} Assembled through alternating, or “layer-by-layer” (LbL), deposition of oppositely charged species, PEM films are clearly different in *form* than naturally occurring cell membranes yet may be designed to confer similar *function*. Through incorporation of enzymes and other proteins,^{25,26} nucleic acids,^{27,28} liposomes,²⁹ biologically active nanoparticles,³⁰ polymers functionalized with

Received: December 20, 2010

Published: April 14, 2011

bioactive motifs,³¹ and guest–host supramolecular complexes,^{32,33} PEM films provide unparalleled opportunities for engineering biologically inspired surfaces for directing cellular behavior and controlling biochemical microenvironments. Moreover, film thickness, permeability, mechanical properties, and surface chemistry may be tailored, providing additional mechanisms for manipulating biophysical phenomenon at interfaces. Hence, the assembly of PEMs directly on cells, cell aggregates, and tissue offers enormous potential for cell surface engineering. However, unlike conventional abiotic glass, ceramic, metallic, or polymeric supports, which are largely passive bystanders of film growth, cell surfaces present complex and dynamic interfaces capable of chemically and physically restructuring in response to film constituents. As such, the well-documented toxicity elicited by most polycations^{34–37} poses a significant hurdle in employing PEMs in cell surface engineering. Therefore, the design of cytocompatible polycations and novel film architectures is critical to successfully exploiting the full potential of PEM capabilities beyond inert substrates and toward viable cells.

Here, we report a new class of PEM film with modular biological functionality and tunable physicochemical properties that can be assembled directly on the surface of living cells and tissues. Toward this end, we have harnessed structure–property relationships to discover a working region in parameter space within which poly(*L*-lysine)-graft-poly(ethylene glycol) (PLL-g-PEG) copolymers undergo a conformational change that mitigates their toxicity while simultaneously facilitating the deposition of PEMs on cell surfaces that can be tailored in composition, reactivity, thickness, and nanomechanical properties. The modularity and versatility afforded by these films is not available from any other current cell surface modification strategy, opening uncharted opportunities in cell engineering and therapeutics. As a clinically relevant and rigorous example, we used PEMs to re-engineer the surface of isolated pancreatic islets, multicellular aggregates containing multiple primary cell types that are responsible for regulating blood glucose levels and have been widely explored as a cell-based therapy for the treatment of diabetes.³⁸ However, widespread clinical application of islet transplantation remains limited by destruction of transplanted cells due to immune rejection,^{38,39} inflammation and thrombosis,^{40,41} hypoxia,^{42,43} and impaired revascularization,^{44,45} among other factors. Re-engineering of islet surfaces with appropriately designed PEM films is well-poised to address such challenges by, for example, encapsulating islets in nanothin conformal coatings,^{46–50} promoting growth of new microvasculature,^{51–53} or serving as a scaffold for bioactive regulators of inflammation and immunity.^{10,16,54–56} Using a murine model of intraportal islet transplantation, we demonstrate the first successful *in vivo* application of PEM-engineered cells, which maintained viability and function upon transplantation into the liver microvasculature and could be used as carriers for localized delivery of PEMs containing a model therapeutic payload. This represents a critical first step toward realizing the potential of cell surface engineering with PEM films in islet transplantation and beyond.

RESULTS AND DISCUSSION

Engineering Cytocompatible Polycations. We, along with others, have previously demonstrated that grafting of poly(ethylene glycol) (PEG) chains can reduce the cytotoxicity of polycations.^{4,34,50} On the basis of such findings, we postulated

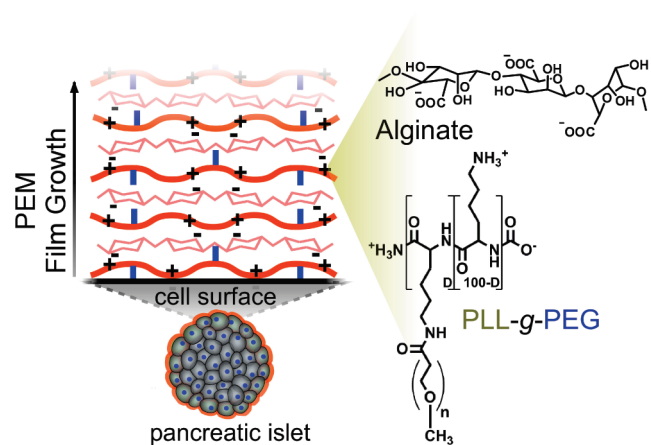


Figure 1. Scheme illustrating the design of cell surface-supported PEM films. Through appropriate control of structural variables, PLL-g-PEG copolymers can be rendered cytocompatible while simultaneously facilitating layer-by-layer self-assembly of PEM films directly on the surface of cells comprising a pancreatic islet. Alginate, a natural and biocompatible polysaccharide, was chosen as the polyanionic species.

that PLL-g-PEG copolymers could be rendered cytocompatible while simultaneously facilitating the assembly of PEM films directly on cell surfaces (Figure 1). However, a considerable challenge in designing such films is the complex interplay between copolymer structural variables that influence cell viability and PEM growth in opposing manners. Notably, decreasing polycation charge density generally attenuates cytotoxicity,³⁷ while insufficiently charged species may be incapable of participating in film growth.^{57,58} Likewise, PLL-g-PEG copolymers with grafted chains of sufficient length can create steric barriers to protein adsorption and molecular recognition⁵⁹ and similarly may hinder electrostatic interactions necessary to drive film assembly. Moreover, polycation molecular weight, conformation, and chemical composition can significantly influence both cytotoxicity^{37,60} and film growth.^{61–63}

In an effort to generate cytocompatible PLL-g-PEG copolymers with maximum positive charge while minimizing potential steric barriers to electrostatic interactions, we synthesized a structural library of 24 PLL_{MW}-g[D]-PEG_n (PMWPn[D]) graft copolymers (Table S1, Supporting Information) comprised of variable PLL backbone molecular weights (PMW), where MW refers to molecular weight in kDa, PEG graft length (Pn), such that n refers to the number of monomeric repeats, and degree of grafting ([D]), defined as the percentage of backbone lysine groups grafted to PEG chains, and assessed islet viability after exposure to copolymers (Figure 2). As expected, polycation toxicity decreased as charge density was reduced (Figure 2b,d), but, interestingly, at a fixed molar concentration and D, increasing PEG graft length decreased cytotoxicity, suggesting synergism between D and Pn in reducing toxicity. As a striking example, grafting of short chains (n = 4) to 43% of lysine residues substantially reduced polycation toxicity relative to a structural analogue with an equivalent fraction of acetylated lysine groups (n = 0). PLL molecular weight also played an important role in cytotoxicity, as otherwise similar copolymers with higher MW backbones were significantly more toxic than their lower MW counterparts (Figure 2c), consistent with previous reports describing an inverse correlation between MW and cytotoxicity.³⁷ Importantly, for each combination of n > 4 and MW explored, a

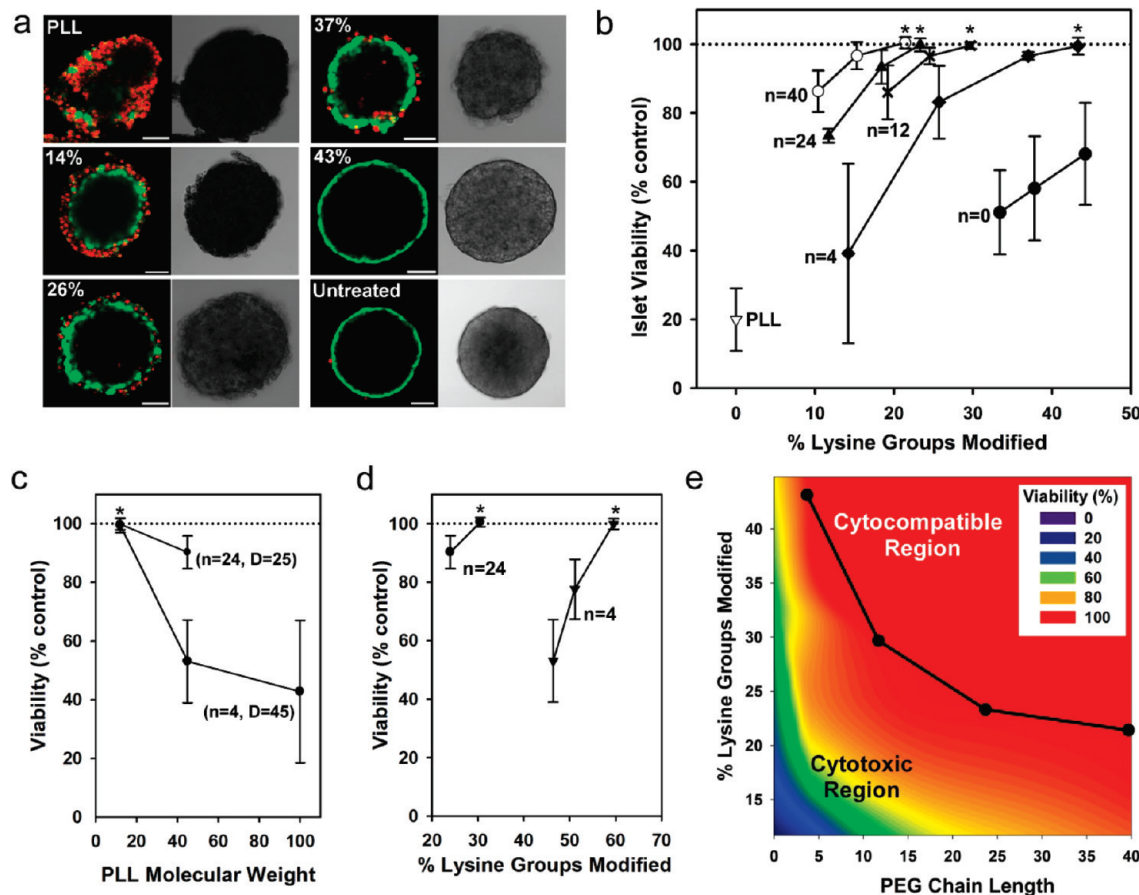


Figure 2. Polycations with enhanced cytocompatibility can be designed by tailoring the structure of PLL-g-PEG copolymers. (a) Representative confocal and bright field micrographs of pancreatic islets stained with calcein AM (green, viable) and ethidium homodimer (red, nonviable) after incubation with 80 μ M PLL and P12P4[D] copolymers with variable degrees (D) of PEG grafting (scale bar, 50 μ m). Polycation toxicity is predominantly exerted toward cells on the periphery of the islet, and the absence of fluorescent emission from the islet core is a consequence of the limited tissue penetration depth of confocal microscopy. (b) Islet viability (mean \pm SD) after exposure to 80 μ M PLL and P12Pn[D] copolymers ($n = 0, 4, 12, 24$, and 40) with variable degrees of PEG grafting. A unique critical degree (D_c) of PEGylation ($*p > 0.05$ vs untreated controls) was observed for each PEG chain length explored (i.e., $n = 4, D_c = 43\%$; $n = 12, D_c = 30\%$; $n = 24, D_c = 23\%$; $n = 40, D_c = 21\%$). (c) For fixed D and n , increasing the PLL backbone molecular weight was found to significantly increase PLL-g-PEG copolymer toxicity. (d) Cytocompatible P45Pn ($n = 4$ and 24) copolymers can be generated by increasing the degree of PEG grafting relative to P12Pn variants ($n = 4, D_c = 60\%$; $n = 24, D_c = 30\%$). (e) Contour plot generated from data in part b demonstrates operative copolymer structure–cytotoxicity relationships, with D_c and n defining a border between cytotoxic and cyocompatible regions in copolymer structure.

critical degree of grafting, D_c , could be identified below which copolymers exerted significant toxicity, thereby defining a maximum permissible charge density for a given composition. As shown in Figure 2a, the small, but statistically significant, decreases in islet viability elicited by some polycations (e.g., P12P4[37]) are a consequence of peripheral cell death. While this may not dramatically influence overall islet viability or function, it is associated with changes in islet morphology, intracellular internalization of film constituents, and eventual loss of dead cells from the islet, all of which compromise the assembly, properties, and utility of cell-surface-supported thin films. For this reason, D_c was defined as the degree of grafting whereby no significant decrease ($p > 0.05$) in islet viability was observed under conditions explored. Relationships between n , D , and cytotoxicity are perhaps most clearly illustrated by the contour plot depicted in Figure 1e generated from viability data collected for P12Pn[D] copolymers. Significantly, this plot demonstrates the existence of a cyocompatible region with a boundary effectively demarcated by D_c and n (overlay), the asymptote of which suggests a maximum permissible backbone charge density of

~80%. It is on this boundary and within this cyocompatible region that copolymers may be explored as candidates that facilitate the assembly of PEM films. While boundaries for larger MW backbones were not explicitly determined, the higher D values mandated for abrogation of cytotoxicity (Figure 2d) reduce the size of the cyocompatible region. For this reason, studies of film assembly focused on P12P4 variants.

Layer-by-Layer Assembly of PEM Films Using PLL-g-PEG Copolymers. Upon identifying cyocompatible copolymer compositions, we next sought to determine if such polycations could facilitate the assembly of PEM films. Alginate, an FDA-approved material that has been widely explored as both a constituent of PEMs and tissue engineered constructs,^{64,65} was selected as the polyanion. To demonstrate assembly of this new class of PEMs, film growth was first investigated with *in situ* ATR-FTIR using P12P4[42] as the polycation. Creation of the desired structure was evidenced by increasing absorbance at 1640 cm^{-1} (amide I, PLL backbone), 1606 cm^{-1} (C=O stretch, alginate), and 1085 cm^{-1} (PEG) with increasing layer number (Figure 3a). A 5

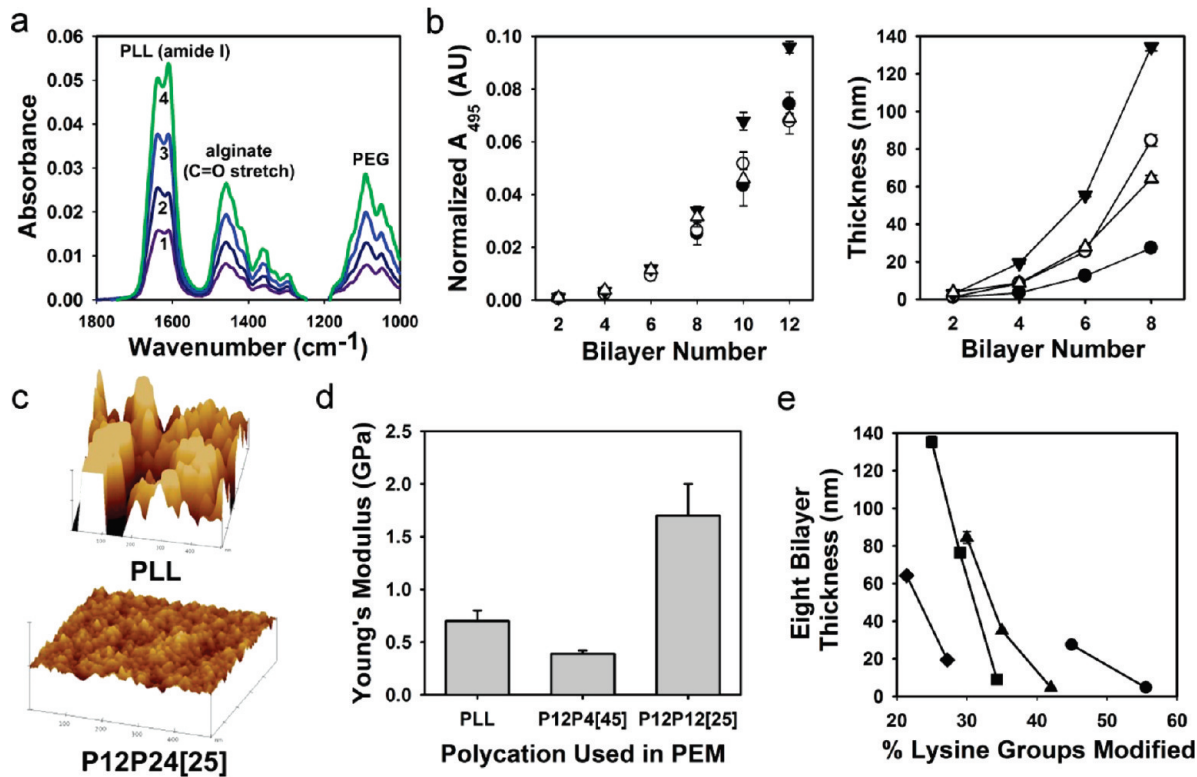


Figure 3. Appropriately structured PLL-g-PEG copolymers facilitate assembly of PEM films with unique and diverse properties. (a) ATR-FTIR spectra of P12P4[42]/alginate PEM film recorded through the first four bilayers. (b) (Left) Absorbance (mean \pm SD) of AlexaFlour488-labeled P12P n [D_c] copolymers as a function of bilayer number measured using solid-state UV-vis spectroscopy. (Right) Ellipsometric film thickness (mean \pm SD) as a function of layer number for films assembled using P12P n [D_c] (●, P12P4[45]; ○, P12P12[30]; ▼, P12P24[25]; △, P12P40[22]). Thickness of selected eight bilayer films was confirmed by the AFM scratch test (Table S2, Supporting Information). (c) Surface topography ($500 \times 500 \text{ nm}^2$; z axis, 5 nm per division) of eight bilayer films assembled using PLL (roughness = 4.6 nm) and P12P24[25] (roughness = 0.28 nm). (d) Young's modulus (mean \pm SD) of dried eight bilayer films assembled with different polycations determined using colloidal probe AFM. (e) Ellipsometric film thickness (mean \pm SD) of eight bilayer films assembled using P12P n copolymers at and above D_c (●, $n = 4$; ▲, $n = 12$; ■, $n = 24$; ◆, $n = 40$).

min deposition time was selected to ensure nearly complete (~98%) polyelectrolyte deposition (Figure S1, Supporting Information), while minimizing exposure of cells to polycations and reducing overall processing time. Employing copolymers of variable charge density, PEG length, and content offers the possibility of generating films with unique and tailorabile properties. Film growth and related properties were investigated on planar substrates by solid-state UV-vis spectroscopy, ellipsometry, and AFM. Solid-state spectroscopy and ellipsometry (Figure 3b) revealed nonlinear, exponential-like growth, with P12P24[25] displaying the steepest profile. Similar profiles have been reported for films assembled using PLL and alginate⁶⁴ or hyaluronic acid⁶⁶ and are distinguished from linear growth by intrafilm diffusion of constituents during assembly,⁶⁶ a phenomenon which could permit polycation–cell interactions even after deposition of a number of layers, further reinforcing the importance of cytocompatible polycations. Moreover, exponential growth generally yields thicker films with hydrogel-like properties that have proven particularly advantageous for loading and locally delivering therapeutic agents.^{25,66} Interestingly, film thickness was highly dependent on the composition of polycation, yielding eight bilayer films that in the dry state ranged from 30 to 135 nm, depending on the choice of copolymer employed. Moreover, the resultant films were remarkably smooth relative to those assembled using PLL (Figure 3c and Table S3, Supporting Information), a characteristic generally associated with films assembled using strongly charged⁶⁷ or stiff polyelectrolytes⁶³ with

important implications for modulating cell adhesion and biocompatibility.⁶⁸ Nanomechanical film properties, measured via colloidal probe AFM, were also dependent on copolymer structure, with P12P24[25] yielding films with a significantly higher Young's modulus than those assembled using PLL or P12P4[45] (Figure 3d), likely a result of independent crystallization of longer PEG chains in the former.⁶⁹ Mechanical properties were measured in the dry state, yielding Young's modulus values between \sim 500 and 1500 MPa, consistent with previous reports describing modulus values of dry films in the range of 1–10 GPa, depending on film components and measurement methods.^{20,70–73} However, it is well-established that increasing the humidity can drastically affect the modulus of PEM films; for example, Rubner and colleagues demonstrated that a film comprised of the weak polyelectrolytes poly(allylamine hydrochloride) and poly(acrylic acid) demonstrated a plain stress Young's modulus of \sim 10 GPa at a relative humidity of 12% while it decreased to \sim 1.1 GPa at 90% humidity.⁷² Additionally, Picart and co-workers have reported Young's modulus values for hydrated, exponentially growing films assembled using PLL and hyaluronic acid in the range of 3–20 kPa.^{74,75} Therefore, the modulus values for PLL/alginate and PLL-g-PEG/alginate PEM films are likely to be significantly lower when hydrated, as is the case on the cell surface, consistent with the hydrogel-like nature of exponentially growing PEM films. Importantly, a cell's fate and behavior are strongly dependent on the mechanical properties of the substrate upon which it adheres,^{76,77} and indeed, the behavior of cells in

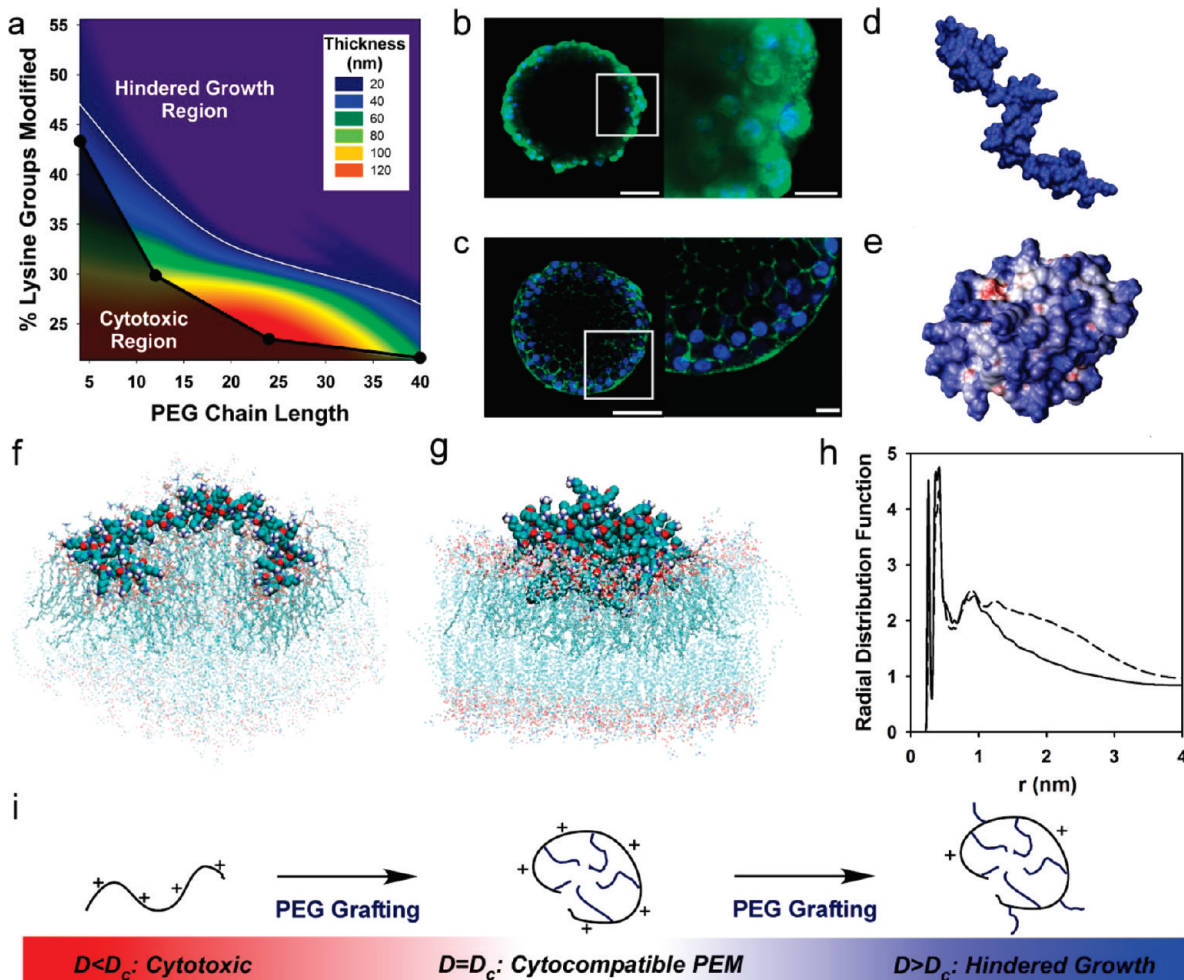


Figure 4. PEG-dependent changes in polycation conformation yield a narrow window within which PEM films can be assembled using cyocompatible copolymers. (a) Contour plot generated with data in Figure 3e demonstrates relationships between film thickness and copolymer structure and predicts a region of hindered film growth (white line, 15 nm contour line). (b) FITC-labeled PLL translocates across cell membranes, whereas (c) AlexaFlour488-labeled P12Pn[D_c] copolymers (shown here, P12P4[45]) remain extracellular and adsorb to cell surfaces [scale bars, 50 μm (left), 10 μm (right)]. Electrostatic potential map of PLL (d) and P12P4[40] (e) at 100 ns (blue; positive charge; red; negative charge; white; neutral). Snapshot of MD simulation at 630 ns for interactions of PLL (f) and P12P4[40] (g) with a 256-lipid POPC lipid bilayer (lipids directly coordinated with PLL (75 lipids) and P12P4[40] (50 lipids) are represented as licorice, and the other lipids are represented as points. PLL and P12P4[40] are represented as VDW; water, Na⁺, and Cl⁻ are not shown). (h) Radial distribution function of P in the PO₄ group of the POPC lipids around PLL (solid line) and P12P4[40] (dashed line) indicates that PLL has a higher coordination with the lipid headgroup of a POPC layer than PLL-g-PEG. (i) Proposed model for describing relationships between polycation conformation, cytotoxicity, and PEM film growth.

contact with PEM films has been found to be highly dependent on modulus in the kilopascal range.^{74,78} Therefore, modulating the stiffness of cell-surface-supported PEMs may offer a unique approach through which to further tailor cellular responses; however, the extent to which hydrated PLL-g-PEG/alginate PEM nanomechanical properties can be modulated has yet to be determined and necessitates further investigation. Nonetheless, whereas other strategies have exploited pH, ionic strength, temperature, and cross-linking agents to modulate film properties, this class of films is unique in that a range of physical properties, including thickness and elastic modulus, may be achieved under physiologically relevant conditions through control of copolymer composition.

PEM film growth was also explored *within* the cyocompatible region by employing P12Pn[D] copolymers with $D > D_c$. For all PEG lengths, increasing D by 5–10% beyond D_c precipitously decreased film thickness, yielding films of only several nanometers after deposition of eight bilayers (Figure 3e). Hence, as

postulated, further decreasing charge density hinders film growth, an effect exacerbated at higher PEG graft lengths, likely owing to generation of steric barriers. Remarkably, between the boundaries of the cytotoxic region and the hindered growth region exists a narrow window within which ultrasmooth films of diverse and unique composition, thickness, and mechanical properties can be generated using cyocompatible polycations (Figure 4a).

Changes in Polycation Conformation Mitigate Cytotoxicity and Facilitate PEM Film Growth. Upon discovering a window of cyocompatible film growth, we sought to explore the molecular basis underpinning its existence. Though not well understood, polycations are thought to elicit toxicity, in part, by inducing nonspecific formation of pores in the plasma membrane, a process dependent on polycation charge density, size, conformation, and chemical composition, among other variables, that results in the unregulated efflux of molecules, including the polycation itself, into the cytoplasm.^{37,60} Indeed, incubation of

islets with FITC-labeled PLL and AlexaFluor488 (AF488)-labeled P12P0[45], both of which are highly cytotoxic, resulted in transport of the polycation across the cell membrane and into the cytoplasm of individual cells (Figure 4b). Conversely, AF488-labeled PMWPn[D_c] copolymers adsorbed to the apical surface of individual cells within pancreatic islets (Figure 4c), indicating maintenance of cell membrane integrity and minimal endocytosis of copolymers. Such contrasting behavior suggests that conjugation of PEG chains to PLL inhibits the capacity of PLL to cross the cell membrane, most likely through inhibition of membrane pore formation, consistent with observed reductions in toxicity.

Molecular modeling has been used to study the molecular mechanisms of polymers interacting with lipid bilayers.^{79–86} Mesoscale thermodynamic models have been used to describe transitions in membrane morphology after exposure to nanoparticles of various size and surface chemistry;⁸⁷ however, such models do not provide detailed molecular interaction mechanisms between particles and the lipid bilayer. The effect of polymer shape and size on membrane pore formation has also been previously studied using coarse-grained molecular dynamics (MD) simulations.^{81–83} However, the experimentally observed disruption of membranes elicited by PLL was not observed in these coarse-grained MD simulations,⁸¹ potentially due to exclusion of the hydrogen effect. Therefore, we chose to use atomic-level MD simulations to elucidate PLL (Figure 4d,f) and P12P4[40] (Figure 4e,g) interactions with a 1-palmitoyl-2-oleyl-sn-glycero-3-phosphocholine (POPC) lipid bilayer as a model cell membrane. We first performed 100 ns simulations to determine the conformational and electrostatic changes to PLL caused by grafting of PEG₄ chains to 40% of lysine residues and subsequently performed 630 ns MD simulations to investigate the interaction characteristics of PLL (Figure 4f) and P12P4[40] (Figure 4g) with the POPC bilayer. The systems were equilibrated after the initial equilibration and the remaining trajectories were used for data analyses (Figures S2 and S3, Supporting Information). Surprisingly, simulations predicted that conjugation of PEG₄ to PLL at 40% grafting ($D = 40$) promotes a conformational switch from an extended random coil ($R_g = 2.3$ nm; Figure 4d, Figure S4a, Supporting Information) to a more globular structure ($R_g = 1.25$ nm) with a PEG-dense core and positively charged corona (Figure 4e, Figure S4b, Supporting Information). To the contrary, Feuz et al. predicted a “bottle brush” conformation for similar PLL-g-PEG copolymers generated through conjugation of a 2 kDa PEG ($n = 40$) to 45% of lysines on a 20 kDa PLL backbone.⁸⁸ This apparent contradiction is likely explained by the different PEG chain lengths employed in the respective models. Longer PEG chains, such as the 2 kDa chains employed by Feuz and colleagues, are highly hydrated and repel each other, giving rise to the more extended “bottle brush” conformation. However, the short tetra(ethylene glycol) (PEG₄) used here has a significantly smaller hydrodynamic radius⁸⁹ and, due to the methoxy headgroup, is less polar^{89,90} than its higher molecular weight counterpart as well as positively charged lysine monomers. Hence, it is reasonable that increased hydrophobicity and reduced steric repulsion would allow P12P4[40] copolymers to adopt the conformation predicted by simulations, which was determined by van der Waals and electrostatic interactions. It should be noted, however, that it was beyond the scope of this work to model all PLL-g-PEG variants employed herein, and therefore, the results of these simulations cannot necessarily be extended to other PLL-g-PEG copolymers.

Upon interaction with a POPC bilayer, PLL (Figure 4f) has a higher affinity for the surface and tends to coordinate with lipid head groups to a greater extent than P12P4[40] (Figure 4g), causing a larger number of lipids to localize around PLL than P12P4[40] (Figure 4f–h). While neither polymer explicitly translocated across the membrane during the initial 630 ns of simulation, which might require even longer simulation times to capture, the enhanced capacity of PLL to interact with and perturb a lipid bilayer supports our experimental findings that PLL has a greater capacity to generate pores in the plasma membrane than copolymers at D_c. These data are also consistent with previous accounts that describe reduced toxicity of polycations with less flexible, more globular conformations.^{36,37}

While simulations were not performed for all structural variants, we postulate that a PEG-dependent conformational switch offers a conceptual model for explaining observed relationships between copolymer structure, cytotoxicity, and PEM film growth (Figure 4i). Below D_c, copolymers lack sufficient PEG grafting to drive a conformational change but maintain a significant degree of positive charge, thereby eliciting membrane pore formation and cytotoxicity. At D_c, a conformational switch occurs, decreasing the capacity of polymers to generate pores in the cell membrane, while retaining a sufficiently high charge density to facilitate PEM film growth. Though MD simulations were only performed for P12P4[40] and results cannot be extrapolated to other variants, it is reasonable that the predicted conformational change would be expected to occur at lower degrees of grafting for longer PEG chains, which are more readily able to interact with each other when spaced further apart along the PLL backbone, thereby decreasing D_c with increased PEG chain length. However, as discussed above, the predicted globular conformation may not persist through all n and D, as the hydration of PEG chains and steric crowding considerations may begin to dominate, causing the chain to adopt a more extended conformation, perhaps explaining the nonlinear relationship between D_c and n. Additionally, the higher entropic penalty attendant to constraining longer PLL backbones in a globular conformation would mandate increased interactions among short PEG chains, potentially explaining the increased toxicity associated with higher molecular weight copolymer variants. With respect to film growth, such globular species are also less apt to unfold to neutralize interfacial negative charges, allowing a sufficient number of lysine residues to remain available for initiating and driving PEM growth.

Above D_c polymers remain cytocompatible, but additional grafting decreases the effective charge of the polymer, thereby hindering interactions with negatively charged surfaces, and hence PEM film growth, a phenomenon potentially exaggerated by steric barriers generated by PEG chains. The ζ -potential of P12P4 copolymers decays rapidly with increasing grafting ratio (Table S4, Supporting Information) and is effectively zero 10% beyond D_c (i.e., P12P4[56]), a polycation which scarcely supported film growth (Figure 3e). Indeed, a critical charge threshold beyond which film growth is no longer possible has been observed in a number of PEM systems.^{57,58} While more extensive simulations of PLL-g-PEG structure and membrane interactions are necessary to fully elucidate relationships between polycation structure, cytotoxicity, and PEM film growth, this working model offers a conceptual molecular framework for the design of cytocompatible polycations for direct assembly of PEM films on cell and tissue surfaces.

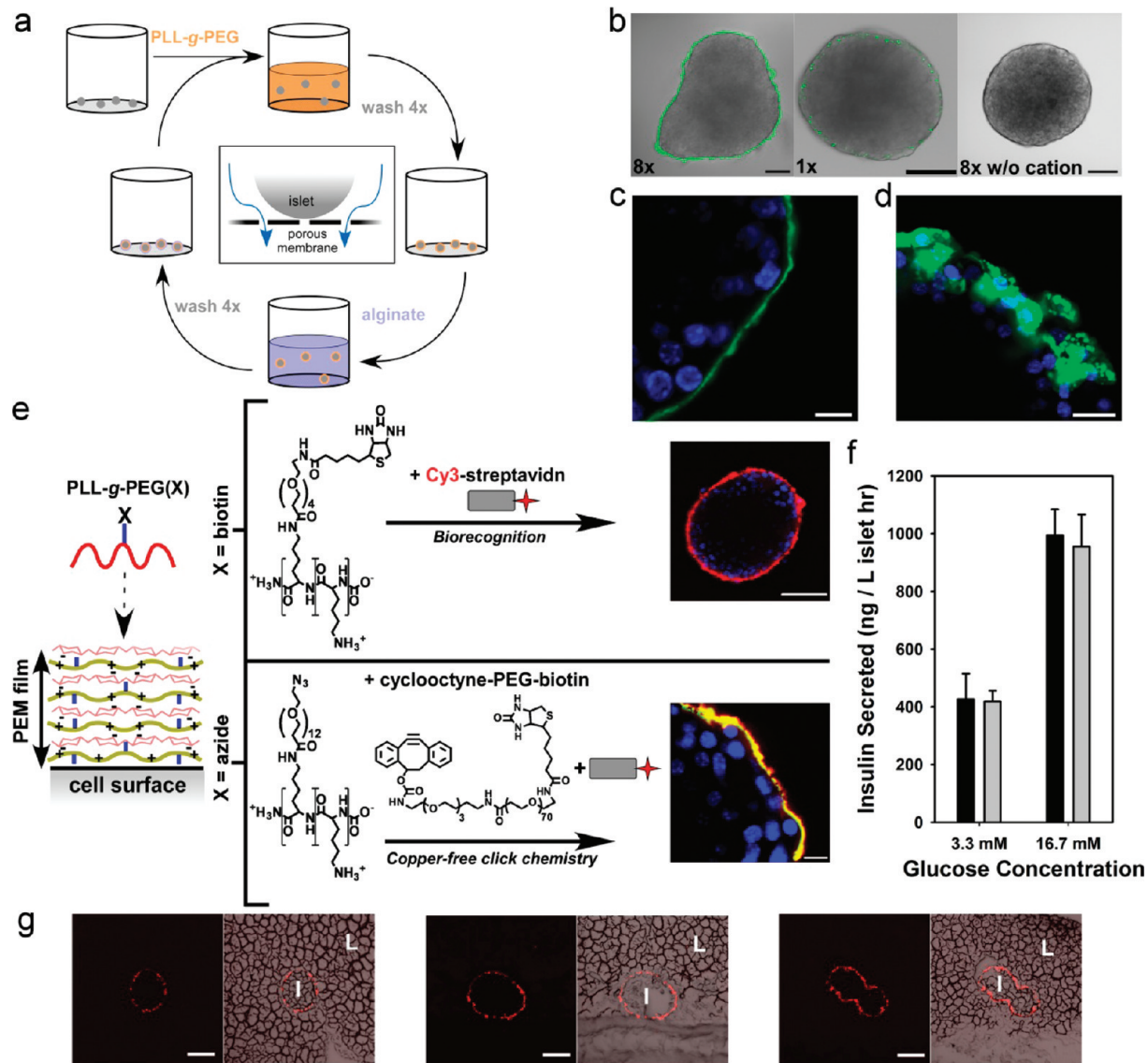


Figure 5. Cell-surface-supported PEMs can be assembled on individual pancreatic islets through LbL deposition of P12Pn[D_c] copolymers and alginate. (a) Method to assemble PEMs on islets. (b) Representative confocal micrographs overlaid on bright-field images of islets coated using P12P24[25] and fluorescein-labeled alginate (F-Alg) with eight bilayers (8×), a single bilayer (1×), or treated only with F-Alg (8× w/o cation). Comparable results were obtained by using P12P4[45], P12P12[30], and P12P40[22]. (c) F-Alg is localized on the extracellular surface of cells, confirming the cell-surface-supported nature of films. (d) By contrast, deposition of a single PLL/F-Alg bilayer resulted in intracellular internalization of alginate by peripheral cells. (e) Chemistry and reactivity of cell-surface-supported PEM films can be tailored through integration of biotin- and azide-functionalized PLL-g-PEG copolymers. (f) Insulin secretion (mean ± SE) by islets coated with a (P12P4[45]/alginate)₈ film (gray bar) and untreated islets (black bar) in response to a step-change in glucose. (g) Confocal (left) overlaid on bright-field micrographs (right) of frozen sections of liver (L) after intraportal transplantation of islets (I) engineered with PEM films labeled with streptavidin–Cy3. Scale bars: b, e (top), g = 50 μm; c, d, e (bottom) = 10 μm.

Engineering Cell Surfaces with PEM Films. Toward assembling PEM films on islets, a process for sequentially depositing polyelectrolytes on cell aggregates was developed (Figure 5a). Islets were placed into cell culture inserts with 12 μm pores, which facilitated drainage of polyelectrolyte and wash solutions while retaining islets (Figure 5a, inset). To form a bilayer, islets were incubated in P12Pn[D_c] copolymers for 5 min, rinsed with serum-free media, incubated in alginate for 5 min, and rinsed again. PEMs were initially assembled using fluorescein-labeled alginate (F-Alg) to enable visualization of films with confocal microscopy and discern differences in fluorescence intensity between islets coated with different numbers of layers. As shown

in Figure 5b, in which P12P24[25] was used as the polycation, a ring of intense fluorescence emanating from F-Alg was observed surrounding the islet periphery. By contrast, controls treated only with F-Alg in an LbL manner demonstrated essentially no fluorescent emission, indicating the necessity of the polycation in immobilizing alginate on the islet surface. Moreover, a dramatic difference in fluorescent intensity was observed between islets coated with eight and one bilayer(s). Collectively, these observations indicate that PEMs can be assembled on the surface of islets via alternating deposition of P12Pn[D_c] copolymers and alginate. In accord with its role as a component of a cell-surface-supported thin film, alginate was concentrated

predominately on the islet surface (Figure 5c). By contrast, attempts to generate a single PLL/F-Alg bilayer resulted in transport of alginate into the cytoplasm (Figure 5d), likely a result of membrane disruption by PLL and subsequent diffusion of alginate across the membrane. Hence, notwithstanding the cytotoxicity of PLL and other polycations, their capacity to generate pores in the cell membrane rather than adsorb to cell surfaces yields intracellular coacervates rather than a surface-supported assembly, an important distinction in light of the different respective properties and applications of each.

The ability to integrate additional molecules into PEM films provides a mechanism for further tailoring film properties and is essential for designing biologically active interfaces. As a demonstration of this concept, cytocompatible PLL-g-PEG copolymers bearing biotin- and azide-functionalized PEG grafts were used as a terminal layer in film assembly to confer biological specificity and chemical reactivity, respectively (Figure 5e). Films assembled with biotin-functionalized copolymers [(P12P4[45]/Alg)₈ + P12P4[45](biotin)] specifically bound Cy3-labeled streptavidin through biorecognition, providing a facile approach to incorporate biotinylated molecules or streptavidin–drug conjugates into cell-surface-supported films. Copper-free click chemistry between azides and cyclooctynes (CyO) is a highly efficient bioorthogonal reaction that proceeds under physiological conditions^{91,92} and, consequently, has recently found utility in cell surface modification and tissue engineering.^{92,93} Indeed, films containing azide-functionalized copolymers [(P12P24/Alg-F)₈ + P12P12[39]-(azide)] selectively captured CyO–PEG–biotin through strain-promoted cycloaddition between the Boons cyclooctyne⁹¹ and azide groups, opening new opportunities for chemoselectively integrating CyO-modified bioconjugates into PEM films. In both cases, control experiments employing nonfunctionalized copolymers demonstrated negligible fluorescence, indicating the bio/chemoselective binding of appropriately functionalized molecules. Though only a terminal deposition of functionalized copolymer was used here, in principle, such conjugates could be integrated at selected points during film formation, conferring spatial control over molecular presentation, allowing, for example, differential functionalization of apical and basal film surfaces and thereby enabling engagement of cell surface receptors while simultaneously presenting bioactive mediators to the environment. While such polycationic vehicles provide a versatile and facile strategy for incorporating diverse molecules and materials into films, other modalities for integrating molecules into PEM films including use of biologically active polyanions,^{28,33} embedding of molecules,^{25,26} and physisorption⁹⁴ may also be explored to further expand the utility of these films.

Importantly, the viability of islets coated with eight bilayer P12Pn[D_c]/alginate PEM films was found to be statistically indistinguishable ($p > 0.01$) from untreated controls both immediately and 18–24 h later after film assembly (Table S5, Supporting Information). Moreover, the functional capacity of islets to release insulin in a glucose-responsive manner was not adversely influenced by film formation, as islets engineered with PEMs secreted statistically similar amounts of insulin at both basal and high glucose concentrations compared to untreated controls ($p > 0.05$; Figure 5f). To demonstrate the potential in vivo application of PEM-engineered cells, islets coated with a model film, (P12P4[45]/alginate)₈/P12P4[45](biotin), functionalized with Cy3-SA, were transplanted into mice through the portal vein and into the liver microvasculature, the clinically preferred site for islet transplantation. As shown in Figure 5g,

fluorescent emission was observed around individual islets distributed throughout the liver, demonstrating the presence of films upon exposure to portal blood and the liver microenvironment. Significantly, these data are the first to demonstrate that PEM-coated cells can be transplanted *in vivo* with a model therapeutic payload. We also explored the effect of PEM film assembly on islet engraftment and function *in vivo* in a model of allogeneic islet transplantation. To accomplish this, islets harvested from B10 mice were coated with a (P12P4[45]/alginate)₈ film and transplanted intraportally into diabetic B6 mice. In this model a suboptimal number of islets are transplanted, resulting in transient reversal of diabetes (euglycemic for >2 consecutive days) in only a fraction of mice during the initial 2 weeks post-transplant. Therefore, different rates of conversion to euglycemia reflect changes in islet survival and function in the immediate post-transplant period. Mice receiving islets coated with the PEM displayed a nearly 2-fold higher rate of conversion from a diabetic to euglycemic state (25% vs 47%; Figure S2, Supporting Information). Significantly, this is the first study to document survival and function of PEM-coated cells or cell aggregates after *in vivo* implantation. Moreover, the observed trend towards improved islet engraftment suggests a potential beneficial effect intrinsic to the film, perhaps through protecting islets from host inflammatory responses. Such beneficial effects are likely to be enhanced through further optimization of film properties and by incorporation of biologically active film constituents that serve to improve islet survival or attenuate inflammatory responses attendant to islet transplantation.

Islet transplantation has long been conceived as a promising treatment for type 1 diabetes,^{95–97} but the challenge of protecting islets from deleterious host responses and environments has limited its potential in the clinic.^{38–40,98,99} Over 30 years of research has led to great progress in the development of cell microencapsulation devices capable of protecting islets from host immune responses while allowing transport of essential nutrients.^{46,100–102} However, the relatively large size of conventional microencapsulation devices can generate consequential mass transport limitations and yield transplant volumes not suitable for infusion into vascularized tissue.^{46,103–105} To address these challenges, several investigators have developed approaches to encapsulate individual islets in coatings that conform to the islet surface, conformal coatings, fabricated using a number of physical and chemical processes.^{46,47,106,107} As shown in Figure 5b, cell surface engineering of islets with PEM films offers opportunities for generating conformal coatings of nanoscale thickness that precisely conform to the geometrically and chemically heterogeneous islet surface. This approach to conformal coating is distinguished from others in that the cell surface serves as the foundation upon which the coating is deposited and grown, allowing thickness and other physicochemical properties to be tailored through control of film constituents and layer number. Moreover, PEM films offer a versatile and facile platform for incorporating diverse biologically active agents into such conformal coatings; indeed, several investigators have improved the efficacy of cell encapsulation devices by integrating molecular regulators of immune responses,^{56,108} inflammation,^{54,109,110} and angiogenesis.¹¹¹ Similarly, several groups have sought to chemically remodel the islet–host interface by, for example, modifying islet surfaces with anti-inflammatory agents,^{10,11} anticoagulants,^{16,55,112} and insulinotropic factors.^{15,113} PEM films offer unparalleled opportunities for creating bioactive interfaces and may open new doors in islet encapsulation and surface modification. Further

exploration of the potential of this technology in islet transplantation and other areas is the subject of ongoing and future research.

CONCLUSION

Cell-based therapies have recently found utility in the treatment of numerous pathologies, including heart and vascular disease, stroke, spinal injury, musculoskeletal disorders, cancer, and diabetes, and cell surface engineering offers great potential to improve clinical outcomes associated with this promising class of therapeutic. Layer-by-layer assembly of PEM films has emerged as among the most versatile, modular, and useful surface engineering approaches, and, hence, is well-poised to greatly expand the molecular repertoire of available cell surface modifications beyond what is currently possible with genetic and metabolic approaches or covalent and noncovalent chemistries. However, this powerful technique has been largely inaccessible to living cell surfaces owing to the toxicity associated with the majority of polycations when in direct contact with the cell membrane. Indeed, in this and previous reports^{4,50} we have demonstrated that polycations conventionally employed for PEM film assembly are highly toxic to pancreatic islets. Here, we have circumvented this molecular hurdle by exploiting PEG-dependent conformational changes in polycation structure to unveil a narrow window in PLL-g-PEG copolymer structure space within which cytocompatible polycations can facilitate the assembly of a unique class of PEM films with tunable biological and physicochemical properties. These films can be assembled directly on the surface of fully viable and functional pancreatic islets via sequential deposition of cytocompatible PLL-g-PEG copolymers and alginate, providing a powerful new platform for engineering cell surfaces layer-by-layer that offers superior versatility and modularity relative to conventional approaches. Furthermore, we have demonstrated the unprecedented use of cells engineered with PEMs *in vivo*, opening exciting possibilities ranging from nanoscale immunoisolation to localized and controlled release of therapeutic molecules from films. Although exemplified in the context of islet transplantation, potential applications are significantly broader in scope, and the extension of this technology to other cell types is poised to offer new opportunities in drug and gene delivery, cell-based therapeutics, imaging, and tissue engineering, efforts which are ongoing in our group. Collectively, these investigations have also provided a conceptual framework for the rational design of cell-surface-supported thin films and establish a new paradigm for translating the numerous and diverse biomedical applications of PEM films from abiotic substrates to living cellular interfaces.

ASSOCIATED CONTENT

S Supporting Information. Detailed Experimental Section, supplemental data, and complete ref 97. This material is available free of charge via the Internet at <http://pubs.acs.org>.

AUTHOR INFORMATION

Corresponding Author
echaikof@bidmc.harvard.edu

ACKNOWLEDGMENT

We are grateful to Prof. Clifford Henderson for assistance with the ellipsometry. This work was supported by grants from the

National Institutes of Health (DK069275) and the Juvenile Diabetes Research Foundation. J.T.W. acknowledges the Whitaker Foundation for generous fellowship support.

REFERENCES

- (1) Saxon, E.; Bertozzi, C. R. *Science* **2000**, *287*, 2007–2010.
- (2) Stephan, M. T.; Moon, J. J.; Um, S. H.; Bershteyn, A.; Irvine, D. J. *Nat. Med.* **2010**, *16*, 1035–41.
- (3) Zhao, W. A.; Teo, G. S. L.; Kumar, N.; Karp, J. M. *Mater. Today* **2010**, *13*, 14–21.
- (4) Wilson, J. T.; Krishnamurthy, V. R.; Cui, W.; Qu, Z.; Chaikof, E. L. *J. Am. Chem. Soc.* **2009**, *131*, 18228–9.
- (5) Contreras, J. L.; Xie, D.; Mays, J.; Smyth, C. A.; Eckstein, C.; Rahemtulla, F. G.; Young, C. J.; Anthony Thompson, J.; Bilbao, G.; Curiel, D. T.; Eckhoff, D. E. *Surgery* **2004**, *136*, 537–47.
- (6) Medof, M. E.; Nagarajan, S.; Tykocinski, M. L. *FASEB J.* **1996**, *10*, 574–86.
- (7) Rabuka, D.; Forstner, M. B.; Groves, J. T.; Bertozzi, C. R. *J. Am. Chem. Soc.* **2008**, *130*, 5947–53.
- (8) De Bank, P. A.; Kellam, B.; Kendall, D. A.; Shakesheff, K. M. *Biotechnol. Bioeng.* **2003**, *81*, 800–8.
- (9) Mahal, L. K.; Bertozzi, C. R. *Chem. Biol.* **1997**, *4*, 415–22.
- (10) Stabler, C. L.; Sun, X. L.; Cui, W.; Wilson, J. T.; Haller, C. A.; Chaikof, E. L. *Bioconjugate Chem.* **2007**, *18*, 1713–5.
- (11) Wilson, J. T.; Haller, C. A.; Qu, Z.; Cui, W.; Urlam, M. K.; Chaikof, E. L. *Acta Biomater.* **2010**, *6*, 1895–903.
- (12) Koyfman, A. Y.; Braun, G. B.; Reich, N. O. *J. Am. Chem. Soc.* **2009**, *131*, 14237–9.
- (13) Sarkar, D.; Vemula, P. K.; Zhao, W. A.; Gupta, A.; Karnik, R.; Karp, J. M. *Biomaterials* **2010**, *31*, 5266–5274.
- (14) Boonyaratpalakorn, S.; Martin, S. E.; Sun, Q.; Peterson, B. R. *J. Am. Chem. Soc.* **2006**, *128*, 11463–70.
- (15) Krishnamurthy, V. R.; Wilson, J. T.; Cui, W.; Song, X.; Lasanajak, Y.; Cummings, R. D.; Chaikof, E. L. *Langmuir* **2010**, *25*, 7675–8.
- (16) Cabric, S.; Sanchez, J.; Lundgren, T.; Foss, A.; Felldin, M.; Kallen, R.; Salmela, K.; Tibell, A.; Tufveson, G.; Larsson, R.; Korsgren, O.; Nilsson, B. *Diabetes* **2007**, *56*, 2008–15.
- (17) Gartner, Z. J.; Bertozzi, C. R. *Proc. Natl. Acad. Sci. U. S. A.* **2009**, *106*, 4606–10.
- (18) Kellam, B.; De Bank, P. A.; Shakesheff, K. M. *Chem. Soc. Rev.* **2003**, *32*, 327–37.
- (19) Decher, G. *Science* **1997**, *277*, 1232–1237.
- (20) Jiang, C. Y.; Markutsya, S.; Pikus, Y.; Tsukruk, V. V. *Nat. Mater.* **2004**, *3*, 721–728.
- (21) Krogman, K. C.; Lowery, J. L.; Zacharia, N. S.; Rutledge, G. C.; Hammond, P. T. *Nat. Mater.* **2009**, *8*, 512–518.
- (22) Hiller, J.; Mendelsohn, J. D.; Rubner, M. F. *Nat. Mater.* **2002**, *1*, 59–63.
- (23) Podsiadlo, P.; Kaushik, A. K.; Arruda, E. M.; Waas, A. M.; Shim, B. S.; Xu, J. D.; Nandivada, H.; Pumplin, B. G.; Lahann, J.; Ramamoorthy, A.; Kotov, N. A. *Science* **2007**, *318*, 80–83.
- (24) Caruso, F.; Caruso, R. A.; Mohwald, H. *Science* **1998**, *282*, 1111–1114.
- (25) Mertz, D.; Vogt, C.; Hemmerle, J.; Mutterer, J.; Ball, V.; Voegel, J. C.; Schaaf, P.; Lavalle, P. *Nat. Mater.* **2009**, *8*, 731–735.
- (26) Shutava, T. G.; Kommireddy, D. S.; Lvov, Y. M. *J. Am. Chem. Soc.* **2006**, *128*, 9926–9934.
- (27) Liu, X. H.; Zhang, J. T.; Lynn, D. M. *Adv. Mater.* **2008**, *20*, 4148–4153.
- (28) Dimitrova, M.; Affolter, C.; Meyer, F.; Nguyen, I.; Richard, D. G.; Schuster, C.; Bartenschlager, R.; Voegel, J. C.; Ogier, J.; Baumert, T. F. *Proc. Natl. Acad. Sci. U. S. A.* **2008**, *105*, 16320–16325.
- (29) Michel, M.; Vautier, D.; Voegel, J. C.; Schaaf, P.; Ball, V. *Langmuir* **2004**, *20*, 4835–4839.
- (30) Yoo, P. J.; Nam, K. T.; Qi, J. F.; Lee, S. K.; Park, J.; Belcher, A. M.; Hammond, P. T. *Nat. Mater.* **2006**, *5*, 234–240.

- (31) Picart, C.; Elkaim, R.; Richert, L.; Audoin, T.; Arntz, Y.; Cardoso, M. D.; Schaaf, P.; Voegel, J. C.; Frisch, B. *Adv. Funct. Mater.* **2005**, *15*, 83–94.
- (32) Benkirane-Jessel, N.; Schwinte, P.; Falvey, P.; Darcy, R.; Haikel, Y.; Schaaf, P.; Voegel, J. C.; Ogier, J. *Adv. Funct. Mater.* **2004**, *14*, 174–182.
- (33) Smith, R. C.; Riollano, M.; Leung, A.; Hammond, P. T. *Angew. Chem.-Int. Ed.* **2009**, *48*, 8974–8977.
- (34) Hunter, A. C. *Adv. Drug Delivery Rev.* **2006**, *58*, 1523–1531.
- (35) Chanana, M.; Gliozzi, A.; Diaspro, A.; Chodnevskaja, I.; Huewel, S.; Moskalenko, V.; Ulrichs, K.; Galla, H. J.; Krol, S. *Nano Lett.* **2005**, *5*, 2605–12.
- (36) Hong, S.; Leroueil, P. R.; Janus, E. K.; Peters, J. L.; Kober, M. M.; Islam, M. T.; Orr, B. G.; Baker, J. R., Jr.; Banaszak Holl, M. M. *Bioconjugate Chem.* **2006**, *17*, 728–34.
- (37) Fischer, D.; Li, Y. X.; Ahlemeyer, B.; Kriegstein, J.; Kissel, T. *Biomaterials* **2003**, *24*, 1121–1131.
- (38) Robertson, R. P. N. *Engl. J. Med.* **2004**, *350*, 694–705.
- (39) Ricordi, C.; Strom, T. B. *Nat. Rev. Immunol.* **2004**, *4*, 259–68.
- (40) Wilson, J. T.; Chaikof, E. L. *J. Diabetes Sci. Technol.* **2008**, *2*, 746–759.
- (41) Bennet, W.; Sundberg, B.; Groth, C. G.; Brendel, M. D.; Brandhorst, D.; Brandhorst, H.; Bretzel, R. G.; Elgue, G.; Larsson, R.; Nilsson, B.; Korsgren, O. *Diabetes* **1999**, *48*, 1907–14.
- (42) Emamallee, J. A.; Shapiro, A. M. *Cell Transplant.* **2007**, *16*, 1–8.
- (43) Lau, J.; Henriksen, J.; Svensson, J.; Carlsson, P. O. *Curr. Opin. Organ Transplant.* **2009**, *14*, 688–693.
- (44) Linn, T.; Schmitz, J.; Hauck-Schmalenberger, I.; Lai, Y.; Bretzel, R. G.; Brandhorst, H.; Brandhorst, D. *Clin. Exp. Immunol.* **2006**, *144*, 179–87.
- (45) Mattsson, G.; Jansson, L.; Carlsson, P. O. *Diabetes* **2002**, *51*, 1362–1366.
- (46) Wilson, J. T.; Chaikof, E. L. *Adv. Drug Delivery Rev.* **2008**, *60*, 124–45.
- (47) Sefton, M. V.; May, M. H.; Lahooti, S.; Babensee, J. E. *J. Controlled Release* **2000**, *65*, 173–86.
- (48) Cruise, G. M.; Hegre, O. D.; Lamberti, F. V.; Hager, S. R.; Hill, R.; Scharp, D. S.; Hubbell, J. A. *Cell Transplant.* **1999**, *8*, 293–306.
- (49) Teramura, Y.; Kaneda, Y.; Iwata, H. *Biomaterials* **2007**, *28*, 4818–25.
- (50) Wilson, J. T.; Cui, W.; Chaikof, E. L. *Nano Lett.* **2008**, *8*, 1940–8.
- (51) Cabric, S.; Sanchez, J.; Johansson, U.; Larsson, R.; Nilsson, B.; Korsgren, O.; Magnusson, P. U. *Tissue Eng. Part A* **2010**, *16*, 961–970.
- (52) Muller, S.; Koenig, G.; Charpiot, A.; Debry, C.; Voegel, J. C.; Lavalle, P.; Vautier, D. *Adv. Funct. Mater.* **2008**, *18*, 1767–1775.
- (53) Chow, L. W.; Wang, L. J.; Kaufman, D. B.; Stupp, S. I. *Biomaterials* **2010**, *31*, 6154–6161.
- (54) Cheung, C. Y.; McCartney, S. J.; Anseth, K. S. *Adv. Funct. Mater.* **2008**, *18*, 3119–3126.
- (55) Totani, T.; Teramura, Y.; Iwata, H. *Biomaterials* **2008**, *29*, 2878–83.
- (56) Hume, P. S.; Anseth, K. S. *Biomaterials* **2010**, *31*, 3166–3174.
- (57) Schoeler, B.; Kumaraswamy, G.; Caruso, F. *Macromolecules* **2002**, *35*, 889–897.
- (58) Glinel, K.; Moussa, A.; Jonas, A. M.; Laschewsky, A. *Langmuir* **2002**, *18*, 1408–1412.
- (59) Huang, N. P.; Michel, R.; Voros, J.; Textor, M.; Hofer, R.; Rossi, A.; Elbert, D. L.; Hubbell, J. A.; Spencer, N. D. *Langmuir* **2001**, *17*, 489–498.
- (60) Leroueil, P. R.; Hong, S.; Mecke, A.; Baker, J. R., Jr.; Orr, B. G.; Banaszak Holl, M. M. *Acc. Chem. Res.* **2007**, *40*, 335–42.
- (61) Kujawa, P.; Moraille, P.; Sanchez, J.; Badia, A.; Winnik, F. M. *J. Am. Chem. Soc.* **2005**, *127*, 9224–9234.
- (62) Podsiadlo, P.; Tang, Z. Y.; Shim, B. S.; Kotov, N. A. *Nano Lett.* **2007**, *7*, 1224–1231.
- (63) Schoeler, B.; Delorme, N.; Doench, I.; Sukhorukov, G. B.; Fery, A.; Glinel, K. *Biomacromolecules* **2006**, *7*, 2065–2071.
- (64) Elbert, D. L.; Herbert, C. B.; Hubbell, J. A. *Langmuir* **1999**, *15*, 5355–5362.
- (65) Choi, N. W.; Cabodi, M.; Held, B.; Gleghorn, J. P.; Bonassar, L. J.; Stroock, A. D. *Nat. Mater.* **2007**, *6*, 908–915.
- (66) Picart, C.; Mutterer, J.; Richert, L.; Luo, Y.; Prestwich, G. D.; Schaaf, P.; Voegel, J. C.; Lavalle, P. *Proc. Natl. Acad. Sci. U. S. A.* **2002**, *99*, 12531–12535.
- (67) McAloney, R. A.; Sinyor, M.; Dudnik, V.; Goh, M. C. *Langmuir* **2001**, *17*, 6655–6663.
- (68) Stevens, M. M.; George, J. H. *Science* **2005**, *310*, 1135–1138.
- (69) Zheng, Y.; Bruening, M. L.; Baker, G. L. *Macromolecules* **2007**, *40*, 8212–8219.
- (70) Tang, Z. Y.; Kotov, N. A.; Magonov, S.; Ozturk, B. *Nat. Mater.* **2003**, *2*, 413–U8.
- (71) Nolte, A. J.; Rubner, M. F.; Cohen, R. E. *Macromolecules* **2005**, *38*, 5367–5370.
- (72) Nolte, A. J.; Treat, N. D.; Cohen, R. E.; Rubner, M. F. *Macromolecules* **2008**, *41*, 5793–5798.
- (73) Pavoor, P. V.; Bellare, A.; Strom, A.; Yang, D. H.; Cohen, R. E. *Macromolecules* **2004**, *37*, 4865–4871.
- (74) Schneider, A.; Francius, G.; Obeid, R.; Schwinte, P.; Hemmerle, J.; Frisch, B.; Schaaf, P.; Voegel, J. C.; Senger, B.; Picart, C. *Langmuir* **2006**, *22*, 1193–1200.
- (75) Richert, L.; Engler, A. J.; Discher, D. E.; Picart, C. *Biomacromolecules* **2004**, *5*, 1908–1916.
- (76) Discher, D. E.; Janmey, P.; Wang, Y. L. *Science* **2005**, *310*, 1139–1143.
- (77) Levental, I.; Georges, P. C.; Janmey, P. A. *Soft Matter* **2007**, *3*, 299–306.
- (78) Ren, K. F.; Crouzier, T.; Roy, C.; Picart, C. *Adv. Funct. Mater.* **2008**, *18*, 1378–1389.
- (79) Lee, H.; Baker, J. R., Jr.; Larson, R. G. *J. Phys. Chem. B* **2006**, *110*, 4014–9.
- (80) Lee, H.; Larson, R. G. *J. Phys. Chem. B* **2006**, *110*, 18204–11.
- (81) Lee, H.; Larson, R. G. *J. Phys. Chem. B* **2008**, *112*, 12279–12285.
- (82) Lee, H.; Larson, R. G. *J. Phys. Chem. B* **2008**, *112*, 7778–84.
- (83) Lee, H.; Larson, R. G. *Molecules* **2009**, *14*, 423–38.
- (84) Lee, H.; Larson, R. G. *J. Phys. Chem. B* **2009**, *113*, 13202–7.
- (85) Illya, G.; Deserno, M. *Biophys. J.* **2008**, *95*, 4163–73.
- (86) Pal, S.; Milano, G.; Roccatano, D. *J. Phys. Chem. B* **2006**, *110*, 26170–9.
- (87) Ginzburg, V. V.; Balijepalli, S. *Nano Lett.* **2007**, *7*, 3716–22.
- (88) Feuz, L.; Leermakers, F. A. M.; Textor, M.; Borisov, O. *Langmuir* **2008**, *24*, 7232–7244.
- (89) Bhat, R.; Timasheff, S. N. *Protein Sci.* **1992**, *1*, 1133–1143.
- (90) Millard, J. W.; Alvarez-Nunez, F. A.; Yalkowsky, S. H. *Int. J. Pharm.* **2002**, *245*, 153–166.
- (91) Ning, X.; Guo, J.; Wolfert, M. A.; Boons, G. J. *Angew. Chem.-Int. Ed.* **2008**, *47*, 2253–5.
- (92) Baskin, J. M.; Prescher, J. A.; Laughlin, S. T.; Agard, N. J.; Chang, P. V.; Miller, I. A.; Lo, A.; Codelli, J. A.; Bertozzi, C. R. *Proc. Natl. Acad. Sci. U. S. A.* **2007**, *104*, 16793–7.
- (93) DeForest, C. A.; Polizzotti, B. D.; Anseth, K. S. *Nat. Mater.* **2009**, *8*, 659–664.
- (94) Kharlampieva, E.; Tsukruk, T.; Slocik, J. M.; Ko, H.; Poulsen, N.; Naik, R. R.; Kroger, N.; Tsukruk, V. V. *Adv. Mater.* **2008**, *20*, 3274–3279.
- (95) Williams, P. *Br. Med. J.* **1894**, *2*, 1303–1304.
- (96) Najarian, J. S.; Sutherland, D. E.; Matas, A. J.; Steffes, M. W.; Simmons, R. L.; Goetz, F. C. *Transplant. Proc.* **1977**, *9*, 233–6.
- (97) Shapiro, A. M.; et al. *N. Engl. J. Med.* **2006**, *355*, 1318–30.
- (98) Shapiro, A. M. J.; Nanji, S. A.; Lakey, J. R. T. *Immunol. Rev.* **2003**, *196*, 219–236.
- (99) Korsgren, O.; Nilsson, B.; Berne, C.; Felldin, M.; Foss, A.; Kallen, R.; Lundgren, T.; Salmela, K.; Tibell, A.; Tufveson, G. *Transplantation* **2005**, *79*, 1289–93.
- (100) Lim, F.; Sun, A. M. *Science* **1980**, *210*, 908–10.
- (101) Lanza, R. P.; Hayes, J. L.; Chick, W. L. *Nat. Biotechnol.* **1996**, *14*, 1107–11.

- (102) Chaikof, E. L. *Annu. Rev. Biomed. Eng.* **1999**, *1*, 103–27.
- (103) Calafiore, R.; Basta, G.; Luca, G.; Lemmi, A.; Montanucci, M. P.; Calabrese, G.; Racanicchi, L.; Mancuso, F.; Brunetti, P. *Diabetes Care* **2006**, *29*, 137–8.
- (104) Leblond, F. A.; Simard, G.; Henley, N.; Rocheleau, B.; Huet, P. M.; Halle, J. P. *Cell Transplant.* **1999**, *8*, 327–37.
- (105) Schneider, S.; von Mach, M. A.; Kraus, O.; Kann, P.; Feilen, P. J. *Artif. Organs* **2003**, *27*, 1053–6.
- (106) Cruise, G. M.; Hegre, O. D.; Scharp, D. S.; Hubbell, J. A. *Biotechnol. Bioeng.* **1998**, *57*, 655–65.
- (107) Teramura, Y.; Iwata, H. *Adv. Drug Delivery Rev.* **2010**, *62*, 827–840.
- (108) Cheung, C. Y.; Anseth, K. S. *Bioconjugate Chem.* **2006**, *17*, 1036–42.
- (109) Ricci, M.; Blasi, P.; Giovagnoli, S.; Rossi, C.; Macchiarulo, G.; Luca, G.; Basta, G.; Calafiore, R. *J. Controlled Release* **2005**, *107*, 395–407.
- (110) Chae, S. Y.; Lee, M.; Kim, S. W.; Bae, Y. H. *Biomaterials* **2004**, *25*, 843–50.
- (111) Lembert, N.; Wesche, J.; Petersen, P.; Doser, M.; Zschocke, P.; Becker, H. D.; Ammon, H. P. *Cell Transplant.* **2005**, *14*, 97–108.
- (112) Teramura, Y.; Iwata, H. *Bioconjugate Chem.* **2008**, *19*, 1389–95.
- (113) Kizilel, S.; Scavone, A.; Liu, X. A.; Nothias, J. M.; Ostrega, D.; Witkowski, P.; Millis, M. *Tissue Eng. Part A* **2010**, *16*, 2217–2228.